

Biosynthesis of Zinc Oxide Nanoparticles Using *Punica granatum* L. Waste Peel Extract, and Assessment of Antioxidant and Catalytic Activity

Mohammad Hadi Meshkatsadat[✉], Alireza Momeni, Mohammad Reza Abdollahzadeh
Department of Chemistry, Qom University of Technology, Iran

✉ Corresponding author. E-mail: meshkatsadat.m@qut.ac.ir

Received: Mar. 9, 2023; **Revised:** Jun. 3, 2023; **Accepted:** Jul. 4, 2023

Citation: M.H. Meshkatsadat, A. Momeni, M.R. Abdollahzadeh. Biosynthesis of zinc oxide nanoparticles using *Punica granatum* L. waste peel extract, and assessment of antioxidant and catalytic activity. *Nano Biomedicine and Engineering*, 2023, 15(4): 378–388.

<http://doi.org/10.26599/NBE.2023.9290030>

Abstract

Green synthesis assisted by plant extracts is a recent research focus in diverse branches of chemistry. Through simple synthesis, different nanoparticles (NPs) can be produced that include oxides of zinc, copper, magnesium, or silver using various types of plant extracts. A remarkable attribute of plant aqueous extracts is their capability to act as reducing and capping agents. This study assessed the antioxidant and catalytic properties of phytosynthesized zinc oxide (ZnO) NPs using the fresh aqueous extract of pomegranate (*Punica granatum*) peel. Scanning electron microscopy indicated that the produced NPs had an average size of 49.52 nm with a spherical shape. X-ray diffraction confirmed the hexagonal phase of ZnO NPs and that their average crystallite size was 41.23 nm according to the Scherrer equation. Analysis of the ultraviolet–visible spectrum was performed to confirm the formation of ZnO NPs, and Fourier transform-infrared analysis illustrated the presence of diverse phytochemicals in the plant extract and ZnO NPs. The 2,2-diphenyl-1-picrylhydrazyl assay was used to determine the radical scavenging activity of these NPs. The novel ZnO phyto-nanocatalyst mediated by extracts from plant waste material, exhibited a well-defined reduction of methylene blue dye. Within 20 min, the catalytic degradation of methylene blue was completed, demonstrating that ZnO NPs have excellent catalytic properties.

Keywords: antioxidant; catalytic degradation; green synthesis; nanoparticles; zinc oxide (ZnO)

Introduction

As a new branch of nanotechnology, the synthesis of metal oxide nanostructures via green approaches has become a focus of recent research [1]. Nanotechnology research has enabled the design of functional systems at the molecular and atomic scale with characteristics similar to those of atoms [1, 2]. Biological and catalytic activity and electrical conductivity properties of NPs are based on unrivaled

characteristics, including large energy–volume ratio of surface area, high proportion of surface atoms, and significant deviation between valence and conduction strip when divided at the near-atomic level, which produces physical and chemical diversity [3].

As a multifunctional nanoparticle (NP), zinc oxide (ZnO) is one of the most highly regarded metallic oxides with a wide band gap (3.37 eV) and a size range of 1–100 nm [4]. The low-cost synthesis, stability, low toxicity, and simple preparation

techniques have made ZnO an appropriate candidate for applications in several fields, including biomedical, catalysis, gas sensors, electronic devices, solar cells, transistors, and photocatalysis. Different methods can be used to produce ZnO nanostructures with varied chemical properties, although several of these are not sufficiently cost-effective for scale-up. Most of these approaches require high energy, expensive shaping reagents, and sophisticated equipment [4, 5]. The use of various low-cost resources, such as the leaves of plants and the seeds and peel of fruit, for the green synthesis of ZnO NPs can produce morphologically diverse species of ZnO NPs. These multifunctional NPs have attracted attention because of their wide range of applications, such as in active ultraviolet sensors, drug delivery, antioxidants, antibacterials, antifungals, environmental remediation, and nutrient sources for crops [6].

The antioxidant and radical scavenging activity of green manufactured ZnO NPs have been compared with chemically manufactured NPs via different tests, including using 2,2-diphenyl-1-picrylhydrazyl (DPPH) and 2,2'-azino-bis(3-ethylbenzothiazoline-6-sulfonic acid) assays [7]. NPs possess strong antioxidant properties because of their size and shape. The most common mechanism for radical scavenging is the production of reactive oxygen species [8]. A further extraordinary feature of ZnO NPs is their catalytic application to degrade water-soluble dyes. Many industries extensively use organic dyes and coloring agents, which are usually disposed of in wastewater [9]. Catalytic studies are commonly conducted using methylene blue (MB), a cationic dye extensively used in textiles; methylene orange, 4-nitrophenol (4-hydroxynitrobenzene), the most widely used herbicide, insecticide, and synthetic dyes; and malachite green and ethidium bromide, which are commonly used dyes for DNA and RNA detection in gels, which can all be degraded by ZnO NPs [10,11]. Utilizing metal oxide catalysts and NaBH_4 , which acts as a reductant agent, is a simple and effective way to degrade MB [12].

Plant and fruit wastes are ideal candidates for both reducing and capping ZnO NPs to produce nontoxic and low-cost products [13, 14]. Pomegranate (*Punica granatum*) peel is an affordable, inexpensive and traditional herbal medicine that has been used in various cultures as an anti-inflammatory, antioxidant, and antihyperglycemic agent [15]. A pomegranate

fruit consists of 60% peel, which is a rich source of flavonoids such as kaempferol 3-O-glucoside, ellagic acid, and monogalloyl hexoside, as well as hydrolysable tannins and many phenolic compounds; and pomegranate peel has been shown to demonstrate radical scavenging activity [16, 17].

This study investigates the ability of ZnO nanocatalysts synthesized from pomegranate peel extract with sodium borohydride (NaBH_4) to remove MB dye from the aqueous environment. The purpose of this study is to produce safe, multifunctional metal oxide NPs that provide a significant increase in radical scavenging activity and dye removal reaction rate. To study the synthesized NPs, we employed several characterization methods, including ultraviolet-visible (UV-Vis) spectrum, scanning electron microscopy (SEM), Fourier transform-infrared (FT-IR), and X-ray diffraction (XRD) analyses.

Experimental

Plant and materials

Fresh pomegranate (*P. granatum*) fruit was collected from Qom province, city of Qom, Iran. Analytically graded metallic salt precursor, zinc sulfate ($\text{Zn}(\text{SO}_4) \cdot 7\text{H}_2\text{O}$), NaOH, NaBH_4 , and MB were purchased from Merck®, Germany.

Pomegranate peels extract preparation

Fresh fruits were collected and peeled to prepare fresh pomegranate peel extract. The fresh peel was washed with tap water and then distilled water to remove all dirt. Afterward, the peels were dried at room temperature under indirect sunlight. To obtain *P. granatum* fresh extract, dried peels were extracted in distilled water at 80 °C for 60 min. The extract was filtered using Whatman filter paper to remove any possible unwanted pieces of peel. For the synthesis of ZnO NPs, the cloudy orange extract of *P. granatum* was stored on a dark, cold shelf.

Phytosynthesis of pomegranate peel extract-mediated ZnO NPs

In a facile and inexpensive approach, 20 mL of fresh peel extract was added drop by drop into a continuously stirring solution of $\text{Zn}(\text{SO}_4)$ at 60 °C. Following 2 h of stirring, 2 mol/L NaOH was added to the solution to stabilize the pH at 12. Phytosynthesis of ZnO NPs by *P. granatum* peel

extract was observed by the apparent change of color to cloudy orange and the formation of precipitate. The precipitates were centrifuged at 6 000 r/min, washed with distilled water and standard ethanol to remove possible impurities. Afterward, the prepared NPs were dried in a hot air oven at 90 °C (Fig. 1).

Characterization of green synthesized ZnO NPs

NP characteristics and their presence in samples were evaluated using UV–Vis spectroscopy, electron dispersive X-ray spectroscopy, FT-IR spectroscopy, and SEM.

The UV–Vis spectrum was analyzed using a Physic-Mini UVS-2500 spectrophotometer with a resolution of 10 nm between 190 and 1 100 nm. The Thermo/Nicolet Avatar 360 FT-IR Spectrometer system was used to record the functional groups of the extract and ZnO NPs in the transmittance mode between 4 000 and 400 cm^{-1} . Radiation emitted from unabsorbed ZnO NPs leaves a specific fingerprint that indicates their characteristics. FT-IR could determine whether plant extracts were effective at reducing oxidation. The imaging of the surface of a sample at the nano- and microscale is performed via SEM to obtain high-resolution images of the structure of the sample. Surface topology of ZnO NPs can be assessed using SEM images by adjusting the density of the electron on the surface and increasing the magnification and field depth [15, 17]. A scanning electron microscope (Tescan Mira 3) was used to examine the surface morphology, crystal size, and shape of ZnO NPs. The crystal structure of ZnO NPs was determined by using a XRD Philips PW1730. Nano-sized particles are represented by the broadening of the XRD pattern. The Debye Scherer's equation ($d = k\lambda/(\beta\cos\theta)$) is used to estimate the average scale of the ZnO NPs [1, 3].

Antioxidant assay

The DPPH test is a common method for measuring radical scavenging activity and uses antioxidants that react with stable DPPH* (deep violet color) to change this to 2,2-diphenyl-2-picrylhydrazine (DPPH:H) that

exhibits yellow discoloration. In the test, 500 μL of 1 mol/L DPPH solution dissolved in 100% methanol was added to different concentrations of ZnO NPs (12.5–250 $\mu\text{g}/\text{mL}$). After being shaken vigorously for 40 min, the mixture was incubated in the dark. Ascorbic acid was used as a control sample during the study. The absorbance of the reactant at 517 nm was measured after incubation. To determine the antioxidant activity of ZnO NPs, the ability to scavenge DPPH was compared with that of ascorbic acid. To ensure the accuracy of the results, a similar test was performed following the initial test conditions.

The free radical scavenging activity percentage (RSA) was calculated using the formula below: $\text{RSA} (\%) = [(A \text{ control} - A \text{ sample}) / A \text{ control}] \times 100$

where A control = absorbance of DPPH without sample; A sample = absorbance of DPPH with sample [18].

Dye degradation assay

The catalytic property of ZnO NPs was tested by using a 30 mL (15 mg/L) sample of textile wastewater contaminated with MB. To assess catalytic activity, 3×10^{-3} g of ZnO NPs and 0.1 mol/L NaBH_4 was added into 2×10^{-5} mol/L MB as a model reaction at pH 10 at room temperature. The decrease in absorbance over time was recorded to investigate the catalytic activity of ZnO NPs in the reduction of MB. The absorbance of MB was recorded every 5 min using a UV–Vis spectrometer (Shimadzu UV-160A) between 450 and 850 nm to study the reduction of the organic dye by ZnO NPs. NPs used to remove MB were re-used to repeat the reaction and were washed with distilled water and dehumidified at 90 °C for 5 min to remove trapped water; ZnO NP properties were not altered by this treatment.

Results and Discussion

Formation of ZnO NPs

Using a few simple steps, green synthesis can

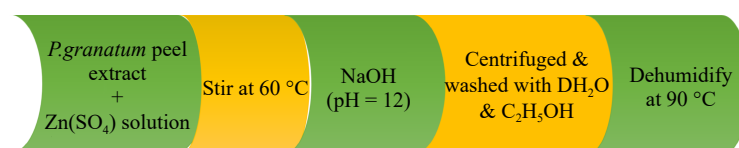


Fig. 1 Schematic of the facile and fast synthesis of ZnO NPs using pomegranate peel extract.

produce metal oxide NPS using chemical precursors and is one of the safest and easiest methods of preparing NPs. Metal precursors can be converted to metal NPs using phytochemicals in plant extracts. Importantly, phytochemicals are antioxidants, which explain why they can act as both reducing and stabilizing agents, as well as being toxic-free chemicals [12]. Terpenoids, flavonoids, phenolic compounds, aldehydes, and alkaloids are essential phytochemicals that contribute to the reduction process. A three-step process encapsulates metal ions with an organic covering to stabilize them after reduction. As the first stage in the process, the activation stage involves reducing metal ions and nucleating these. During the first reduction phase, Zn ions (Zn^{2+}) are converted to Zn^{1+} , and finally to ZnO. Upon completion of the growth phase, the NPs will be stable, and the termination phase will determine the shape of the particle [19].

Characterization of ZnO NPs

UV–Vis

UV–Vis spectrophotometry is a valid technique to confirm the formation of NPs. Most of the NPs are observed in the electromagnetic wave region between 200 and 700 nm [20], and the specified peaks of ZnO NPs are generally between 289 and 385 nm [21, 22]. By stimulating ZnO NPs surface plasmon resonance, a visible color change is caused. The ZnO NPs synthesized with the *P. granatum* peel extract showed a specific peak at 350 nm (Fig. 2(a)), which was compared with other ZnO NPs produced by fruit peel extracts (Table 1) [23–27]. Furthermore, the UV–Vis spectrum of pomegranate peel extract showed a peak at 379 nm, which previous studies have defined as an indication of phenolic compounds present in the pomegranate peel extract [22]. By using the bandgap Tauc plot calculation also, the bandgap was determined as 3.26 eV (Fig. 2(b)).

FT-IR

FT-IR spectroscopy is the most effective method to investigate the functional groups in charge of the reduction process and helps to specify the efficiency of plant extracts as reducing agents [27, 28]. The chemistry and associated functional group variations to ZnO NPs surface can be identified by FT-IR [29]. Lucrative functional groups in biomolecules in

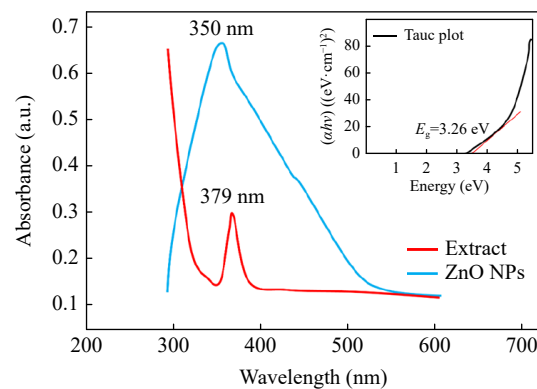


Fig. 2 UV–Vis spectrum of ZnO NPs (blue) and *P. granatum* peel extract (red). Energy band gap Tauc plot.

Table 1 UV wavelength comparison of ZnO NPs prepared using different fruit peel extracts

Fruit	Wavelength (nm)	Reference
<i>Actinidia deliciosa</i>	362	[23]
<i>Banana</i>	315–350	[24]
<i>Citrus sinensis</i>	370	[25]
<i>Hylocereus polyrhizus</i>	369	[26]
<i>Hylocereus undatus</i>	360	[27]
<i>P. granatum</i>	350	Present study

extracts include –O–H, C=O, C=C, C–N, C–H, and N–H can be detected in FT-IR analysis [30]. As shown in Fig. 3, the FT-IR spectra of ZnO NPs powder displayed numerous absorption peaks at 3 434, 1 634.77, 1 383.27, 1 357.32, 1 081.64, and 497.34 cm^{-1} . A wide peak at 3 434 cm^{-1} is defined by the presence of hydroxyl groups (O–H) present in the capping agent. The peak at 1 634.77 cm^{-1} represents the C=C frequency. The peak at 1 383.27 cm^{-1} is attributed to the symmetric stretching of the carbonyl side groups found in capping and stabilizing agents. The peak at 497.34 cm^{-1} indicates the stretching frequency of ZnO NPs. Functional groups found in phytochemicals have a strong affinity toward Zn ions

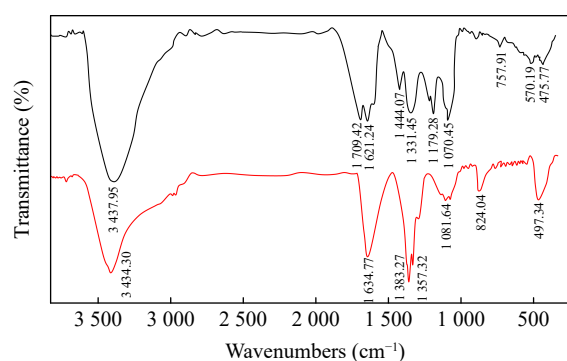


Fig. 3 FT-IR spectrum of *P. granatum* peel extract (black) and ZnO NPs (red).

and probably contribute to the formation of ZnO NPs. Furthermore, phytochemicals cause ZnO NPs to coalesce to stabilize and cap them.

XRD analysis

Sample crystallinity is defined with the XRD analysis technique. The degree of crystallinity and the difference of a particular element in relation to its ideal composition and structural condition, may also be inferred from this analysis. The interaction of the X-ray beam with the atomic planes gives rise to partial transmission of the beam while the remaining radiation is absorbed, refracted, scattered, and diffracted by the sample. Each element diffracts the X-ray differently depending on its atomic arrangement and type of atoms. Moreover, the hexagonal common crystal structure of the ZnO NPs is attributed to its related face velocities and crystal symmetry [31]. The ZnO NPs were penetrated by X-rays and scanned across the region of 2θ , between 0° and 80° . As shown in Fig. 4, the peaks were hexagonal and almost in accordance with the reported data (jcpds-79-0206). Specific reflections were present at 31.87° , 34.43° , 36.13° , 47.24° , 56.62° , 62.85° , 67.8° , and 69.02° corresponding to (100), (002), (101), (102), (110), (103), (112), and (201) orientations respectively. The diffractograms did not show any peaks associated with the secondary phase or impurities. The polycrystalline structures of the ZnO NPs are clearly visible in the peak at (101). Using the Debye–Scherrer equation ($D = 0.9\lambda/(\beta\cos\theta)$) where λ is the X-ray wavelength (generally 1.5406 \AA), β is full width at half maximum of the peak located at 2θ , and θ is the Bragg angle of diffraction, the average crystallite size of ZnO NPs was calculated to be 41.23 nm .

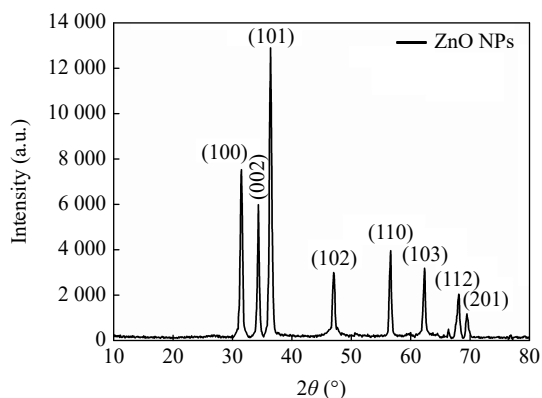


Fig. 4 ZnO NPs XRD pattern.

SEM

SEM was used to determine the surface morphology, size, and shape of the green synthesized ZnO NPs (Fig. 5) [17]. The detector produces and records signals from electron beams to ZnO NPs [32]. Analysis of thin films of samples was performed on carbon-coated copper grids prepared by dropping a very small quantity of sample over the grid. SEM characterization of ZnO NPs revealed a spherical shape and size range of $27\text{--}99 \text{ nm}$ and an average particle size of 49.52 nm ; a comparison of shape and size of ZnO NPs produced by other fruit peel extracts is shown in Table 2 [22, 25–26, 32–33]. Moreover, the NP size distribution diagrams (Fig. 6) show that 55% of NPs were between 27 and 45 nm , with only about 10% of the NPs having dimensions between 81 and 99 nm . According to this diagram, most NPs are designed with dimensions $<50 \text{ nm}$, which can enhance their performance in organic dye removal and radical scavenging.

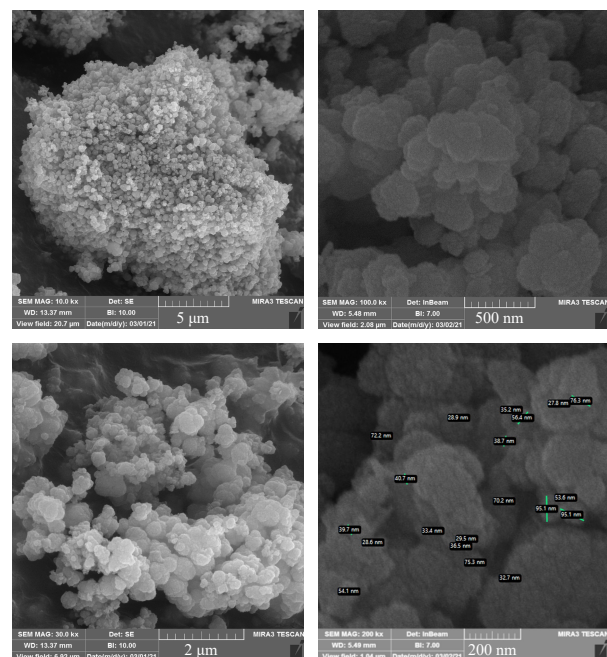


Fig. 5 SEM images of ZnO NPs and size average chart.

DPPH test and antioxidant activity of ZnO NPs

The DPPH test is a common method to determine the ability of radical scavenging in synthesized NPs [34, 35]. The DPPH scavenging activity of ZnO NPs synthesized with *P. granatum* peel extract was compared with that of ascorbic acid (Fig. 7). The ZnO NPs exhibited the highest radical scavenging activity at a concentration of $200 \mu\text{g/mL}$, exceeding ascorbic

Table 2 Morphological and size comparison of fruit peel extract-mediated ZnO NPs

Fruit	Particle size (nm)	Shape	Reference
<i>Actinidia deliciosa</i>	8.2	spherical and hexagonal	[22]
<i>Hylocereus polyrhizus</i>	52.5	spherical	[25]
<i>Hylocereus undatus</i>	70	spherical	[26]
<i>Citrus aurantifolia</i>	50	spot-like	[32]
<i>Pithecellobium dulce</i>	30	spherical	[33]
<i>P. granatum</i>	49.52	spherical	Present study

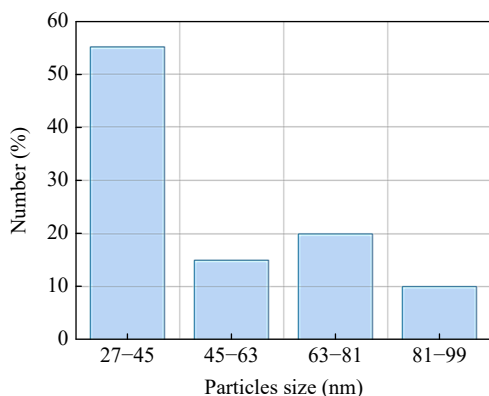


Fig. 6 Particle size distribution of ZnO NPs.

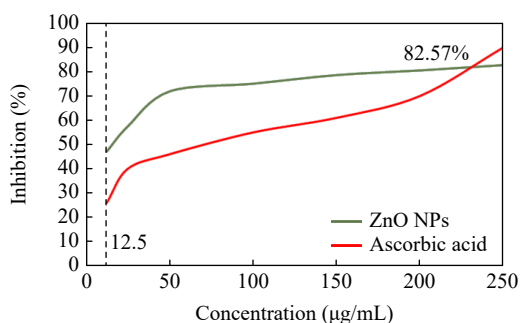


Fig. 7 DPPH scavenging activity comparison between ZnO NPs and ascorbic acid.

acid in this regard. Table 3 shows the antioxidant activity of ZnO NPs synthesized from *P. granatum* peel extract.

Table 3 Antioxidant activity (% of inhibition) of ZnO NPs

Concentration (µg/mL)	Ascorbic acid(Control)	ZnO NPs (<i>P. granatum</i> -mediated)
12.5	26	47.16
50	46	71.78
100	55	74.94
150	61	78.48
200	70	80.39
250	90	82.57

Catalytic activity of ZnO NPs

ZnO NPs were investigated for their catalytic activity

using MB as a dyestuff model with NaBH₄ as a reducing agent and monitoring of the reduction through a UV-Vis spectrophotometer. During the test, MB, which exhibits a characteristic absorption peak at 670 nm, is reduced to leuco-MB.

As part of the study to investigate what effect NaBH₄ may have as a catalyst and whether it can degrade organic dye, two samples were prepared, one in the presence of the catalyst and NaBH₄ and one with NaBH₄ only. The spectral analysis indicates that the reaction occurred rapidly in the presence of ZnO nanocatalyst and was completed with a 90% reduction of MB in 20 min compared with the 5% reduction of MB in the absence of a catalyst (Fig. 8).

Figure 9 illustrates the UV-Vis spectrum of MB reduction in the presence of ZnO NPs. In addition, the

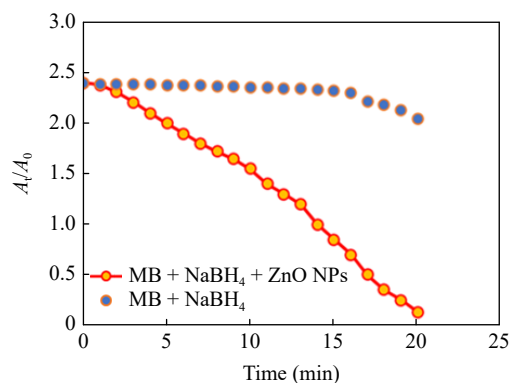


Fig. 8 Spectral analysis of presence and absence of ZnO NPs in MB reduction.

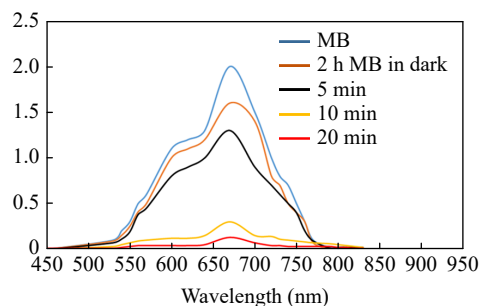
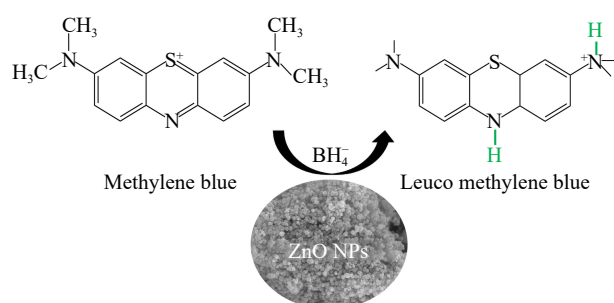


Fig. 9 Successive reduction of MB by ZnO NPs.

Table 4 Comparison of the catalytic activity of distinct NPs with ZnO mediated by *P. granatum* peel extract

NP	Plant name	Target pollutant	Degradation	Degradation Time (min)	Reference
ZnO	<i>Conyza canadensis</i>	Methylene blue	85.3%	20	[18]
Au (Gold)	<i>Nigella arvensis</i>	Methylene blue	44%	2880	[36]
Ag (Silver)	<i>Costus Pictus</i>	Methylene blue	85%	316	[37]
Au (Gold)	<i>Costus Pictus</i>	Methylene blue	42%	—	[37]
ZnO	<i>P. granatum</i>	Methylene blue	90%	20	Present study

spectrum of MB and saturated MB in darkness is shown. By demonstrating that 90% of MB could be reduced in 20 min using ZnO NPs, this study clearly confirms the efficiency of the catalytic reduction of MB by green synthesized nanocatalysts. Table 4 summarizes the MB degradation achieved using different NPs. Figure 10 illustrates the relevant mechanism of MB degradation whereby the organic dye is converted into CO₂ and inorganic ions.

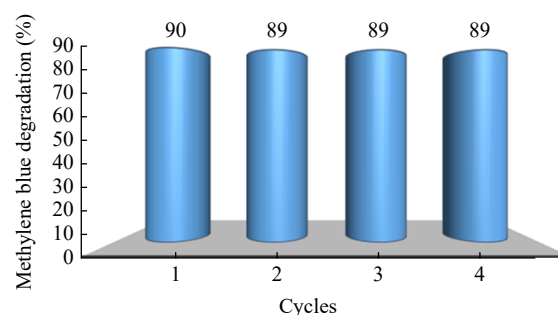
**Fig. 10** Relevant mechanism of degradation of methylene blue by ZnO NPs.

Environmentally friendly catalytic procedures are highly desirable, preferably in aqueous environments. Avoiding the use of volatile organic solvents, NaBH₄ is a preferred water-soluble reducing agent for representative reductions, and an organic color reduction can be justified based on the electron transfer. ZnO, as a semiconductor, can efficiently transfer electrons between receptors and donors. Consequently, electrons will be transferred to the receptor (MB) with the help of the donor (BH₄⁻). Initially, the dye and NaBH₄ molecules are absorbed onto the surface of ZnO NPs. Upon absorption, NaBH₄ becomes a strong nucleophilic agent, and the dye acts as an electrophilic agent. In the solution, ZnO NPs function as relay systems to assist in the transfer of electrons required for the dye degradation process from NaBH₄ to the organic dye molecules. A dye molecule is degraded into small colorless products including CO₂, H₂O, and SO₄²⁻. This process converts MB to leuco-MB [35, 37–39].

The presence of effective substances and phytochemicals on the surface of NPs prevents the uncontrollable growth of the particle size as a stabilizing agent and the accumulation and adhesion of NPs to each other. The first important effect of phytochemicals on the catalytic activity of NPs is to maintain and limit the size of nanocatalysts, and by creating stability, the nanocatalysts can be reused [40]. In addition, by preventing NPs from aggregating and increasing the ratio of surface area to volume, the number of active sites increases. Consequently, NPs can transfer more electrons from the acceptor (organic dye) to the donor (borohydride). Therefore, the presence of active substances and phytochemicals at the surface of NPs increased the catalytic properties of the NPs. Furthermore, with the stability promoted by the capping agents, the pollutant dye is removed more quickly [41].

Recyclability of nanocatalysts

It is important that a catalyst demonstrates both high activity and stability when used at a large scale. Therefore, the ZnO NPs were re-used to degrade MB for four consecutive cycles to determine the efficiency of their recycling, and no significant loss of catalytic activity was observed after these four successive rounds of degradation (Fig. 11).

**Fig. 11** Degradation cycle efficiency.

FT-IR, XRD, and SEM analyses were also performed to ensure that the physical and chemical properties of the nanocatalyst were maintained after

the four successive cycles. No transfer or identified change in the chemical properties of NPs occurred, and the FT-IR spectrum of recycled ZnO NPs remained similar to the spectrum of NPs before the organic dye removal reaction (Fig. 12). In the FT-IR spectra, the peaks of various functional groups, such as C–O, C=O, and C–H bonds, were still present in the NP samples, and no significant shifts were observed. Thus, NPs remained in their original chemical form. In addition, XRD analysis was performed to compare two unused and recycled samples (Fig. 13). The NPs retained significant stability by maintaining their crystalline phase and size corresponding to hexagonal shape in accordance with the reported data (jcpds-79-0206).

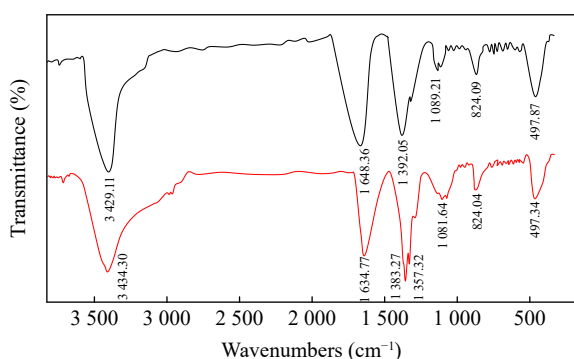


Fig. 12 Comparison of FT-IR spectrum of unused (red) and recycled (black) ZnO NPs.

Thus, the NPs were not significantly affected by the recycling process and their physical characteristics remained intact even after multiple uses. This indicates that ZnO NPs are highly stable, which makes them ideal for various applications.

To assess the morphological stability of the recycled nanocatalysts, field emission-SEM images were prepared to ensure that the biosynthesized nanocatalysts retained their original shape and size. The NPs were spherical and their dimensions were between 32 and 70 nm, with an average size of 59.94 nm (Fig. 14). Therefore, the nanocatalyst retains its physical and chemical properties. In addition, the synthesis method allowed for the reuse of the nanocatalyst and the ability to recover and recycle the catalytic material, making this a sustainable approach. Notably, by maintaining properties and recyclability, these NPs follow all 12 principles of green chemistry.

The performance and activity of the ZnO NPs in removing MB dye from water environments are

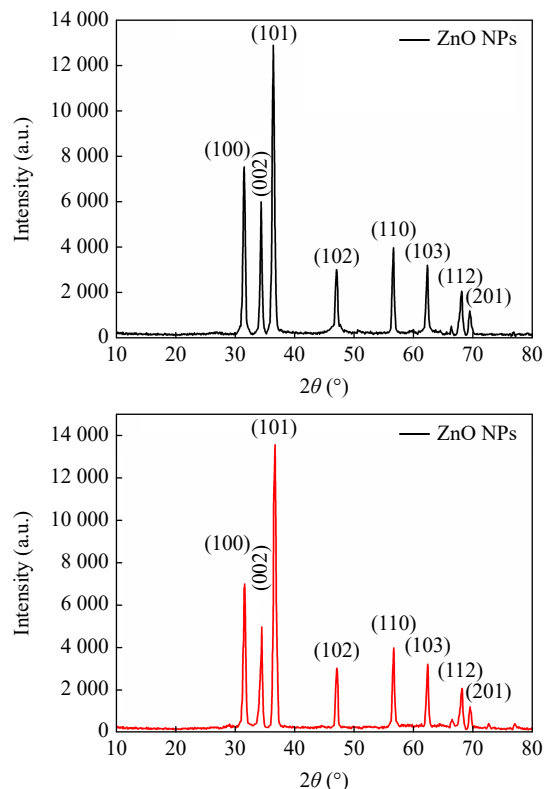


Fig. 13 XRD pattern of unused (black) and recycled (red) ZnO NPs.

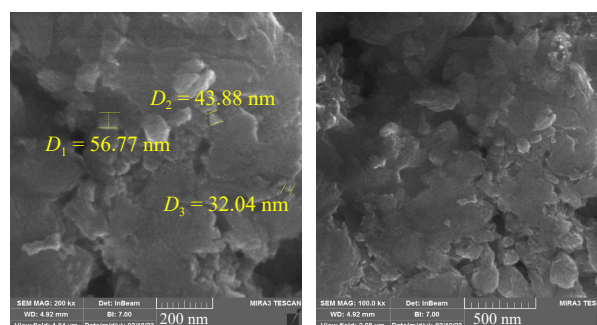


Fig. 14 Field emission-SEM image of recycled ZnO NPs.

influenced by the dimensions of the NPs and their surface-to-volume ratio. Additionally, their spherical shape and appropriate dimensions provide them with an optimal chance of absorbing dye onto the nanocatalyst surface. Biomolecules on NP surfaces increase their antioxidant activity, because of the use of active ingredients in this synthesis, and in this case, pomegranate peel extract, which is a rich source of biomolecules. Compared with vitamin C, which is a strong antioxidant, phytosynthesized ZnO NPs are more effective at lower concentrations in radical scavenging. The produced NPs in this study are derived from natural sources and are economical and safe and thus can be mass produced; therefore, these NPs may help produce significant developments in the biomedical and environmental fields and

contribute to the preservation of the environment and human health. Multifunctional ZnO NPs could be synthesized by conducting further studies on phytosynthesized NPs described here, utilizing previous research outcomes and optimizing them. This would help advance the use of green synthesis in nanotechnology and encourage other researchers to conduct safer and environmentally friendly studies.

Conclusion

This study developed an efficient, cost-effective, and sustainable method for ZnO NPs phytosynthesis using pomegranate peel extract. Based on the 12 green chemistry principles, no harmful solutions or substances were used in this study, and the final product was also recyclable and reusable. Typically, plant leaf extract is used in green synthesis of metal oxide NPs, although mass production of these NPs is prevented because of biodiversity protection concerns and the extinction of rare species. This study, make good use of pomegranate peel extract, a plant waste material that contains beneficial compounds and active substances suitable for biosynthesis. Based on FT-IR and UV-Vis spectrophotometry, the extract used in this study reduces Zn ions and stabilizes ZnO NPs, proving that waste materials can be used to synthesize metal oxide NPs with unique properties. In view of the physicochemical properties of these NPs and their practical dimensions and structure, which are <100 nm and hexagonal, the ability to remove MB from an aqueous environment in a short period of time is a very promising usage in this field. These NPs also exhibited more antioxidant properties than those of ascorbic acid, a strong antioxidant, at low concentrations and up to 200 µg/mL. Accordingly, phytosynthesized ZnO NPs from pomegranate peel extract are multifunctional and competitive NPs because of their radical scavenging abilities, in addition to the color removal property using only NaBH₄.

CRedit Author Statement

Mohammad Hadi Meshkatsadat: antioxidant data analysis, writing–review, and experimental studies. **Alireza Momeni:** writing original draft, catalytic data analysis, and revision. **Mohammad Reza Abdollahzadeh:** funding acquisition and software.

Acknowledgement

Authors are thankful to the Department of Chemistry and deputy of research of Qom University of Technology for technical support in this project.

Conflict of Interest

All authors declare that there is no conflict of interest.

References

- [1] K, Nithya, S. Kalyanasundharam. Effect of chemically synthesis compared to biosynthesized ZnO nanoparticles using aqueous extract of *C. halicacabum* and their antibacterial activity. *OpenNano*, 2019, 4: 100024. <https://doi.org/10.1016/j.onano.2018.10.001>
- [2] H. Chemingui, T. Missaoui, J. Chékir-Mzali, et al. Facile green synthesis of zinc oxide nanoparticles (ZnO NPs): Antibacterial and photocatalytic activities. *Materials Research Express*, 2019, 6(10): 1050b4. <https://doi.org/10.1088/2053-1591/ab3cd6>
- [3] S. Yedurkar, C. Maurya, P. Mahanwar. Biosynthesis of zinc oxide nanoparticles using *Ixora coccinea* leaf extract—a green approach. *Open Journal of Synthesis Theory and Applications*, 2016, 5(1): 1–14. <https://doi.org/10.4236/ojsta.2016.51001>
- [4] A. Santhoshkumar, H.P. Kavitha, R. Suresh, et al. ZnO nanoparticles: Hydrothermal synthesis and 4-nitrophenol sensing property. *Journal of Materials Science: Materials in Electronics*, 2017, 28(13): 9272–9278. <https://doi.org/10.1007/s10854-017-6663-6>
- [5] J. Perelaer, P.J. Smith, D. Mager, et al. Printed electronics: The challenges involved in printing devices, interconnects, and contacts based on inorganic materials. *Journal of Materials Chemistry*, 2010, 20(39): 8446. <https://doi.org/10.1039/C0JM00264J>
- [6] A. Mohanan Pillai, V.S. Sivasankarapillai, A. Rahdar, et al. Green synthesis and characterization of zinc oxide nanoparticles with antibacterial and antifungal activity. *Journal of Molecular Structure*, 2020, 1211: 128107. <https://doi.org/10.1016/j.molstruc.2020.128107>
- [7] D. Rehana, D. Mahendiran, R.S. Kumar, et al. *In vitro* antioxidant and antidiabetic activities of zinc oxide nanoparticles synthesized using different plant extracts. *Bioprocess and Biosystems Engineering*, 2017, 40(6): 943–957. <https://doi.org/10.1007/s00449-017-1758-2>
- [8] A. Avalos, A.I. Haza, D. Mateo, et al. Cytotoxicity and ROS production of manufactured silver nanoparticles of different sizes in hepatoma and leukemia cells. *Journal of Applied Toxicology*, 2014, 34(4): 413–423. <https://doi.org/10.1002/jat.2957>
- [9] K. Elumalai, S. Velmurugan, S. Ravi, et al. Bio-approach: Plant mediated synthesis of ZnO nanoparticles and their catalytic reduction of methylene blue and antimicrobial activity. *Advanced Powder Technology*, 2015, 26(6): 1639–1651. <https://doi.org/10.1016/j.apt.2015.09.008>
- [10] K.M. Omer, N.N. Mohammad, S.O. Baban. Up-conversion fluorescence of phosphorous and nitrogen Co-doped carbon quantum dots (CDs) coupled with weak

- LED light source for full-spectrum driven photocatalytic degradation via ZnO-CDs nanocomposites. *Catalysis Letters*, 2018, 148(9): 2746–2755. <https://doi.org/10.1007/s10562-018-2459-4>
- [11] M.N. Alharthi, I. Ismail, S. Bellucci, et al. Biosynthesis microwave-assisted of zinc oxide nanoparticles with *Ziziphus jujuba* leaves extract: Characterization and photocatalytic application. *Nanomaterials*, 2021, 11(7): 1682. <https://doi.org/10.3390/nano11071682>
- [12] J. Singh, T. Dutta, K.H. Kim, et al. 'Green' synthesis of metals and their oxide nanoparticles: Applications for environmental remediation. *Journal of Nanobiotechnology*, 2018, 16(1): 84. <https://doi.org/10.1186/s12951-018-0408-4>
- [13] J. Qu, X. Yuan, X. Wang, et al. Zinc accumulation and synthesis of ZnO nanoparticles using *Physalis alkekengi* L. *Environmental Pollution*, 2011, 159: 1783–1788. <https://doi.org/10.1016/j.envpol.2011.04.016>
- [14] D.S. Auld. Zinc coordination sphere in biochemical zinc sites. *Biometals*, 2011, 14: 271–313. <https://doi.org/10.1023/a:1012976615056>
- [15] L. Tamborlin, B.R. Sumere, M.C. de Souza, et al. Characterization of pomegranate peel extracts obtained using different solvents and their effects on cell cycle and apoptosis in leukemia cells. *Food Science & Nutrition*, 2020, 8(1): 5483–5496. <https://doi.org/10.1002/fsn3.1831>
- [16] W.M. Husain, J.K. Araak, O.M. Ibrahim. Green Synthesis of Zinc oxide nanoparticles from (*Punica granatum* L) pomegranate aqueous peel extract. *The Iraqi Journal of Veterinary Medicine*, 2022, 43(20): 6–14. <https://doi.org/10.30539/iraqijvm.v43i2.524>
- [17] P. Ambigaipalan, A.C. de Camargo, F. Shahidi. Phenolic compounds of pomegranate byproducts (outer skin, mesocarp, divider membrane) and their antioxidant activities. *Journal of Agricultural and Food Chemistry*, 2016, 64(34): 6584–6604. <https://doi.org/10.1021/acs.jafc.6b02950>
- [18] L.B. Du, S. Suo, G.Q. Wang, et al. Mechanism and cellular kinetic studies of the enhancement of antioxidant activity by using surface-functionalized gold nanoparticles. *Chemistry - A European Journal*, 2013, 19(4): 1281–1287. <https://doi.org/10.1002/chem.201203506>
- [19] A.J. Love, V.V. Makarov, O.V. Sinitsyna, et al. A genetically modified tobacco mosaic virus that can produce gold nanoparticles from a metal salt precursor. *Frontiers in Plant Science*, 2015, 6: 984. <https://doi.org/10.3389/fpls.2015.00984>
- [20] P. Jamdagni, P. Khatri, J.S. Rana. Green synthesis of zinc oxide nanoparticles using flower extract of *Nyctanthes arbortristis* and their antifungal activity. *Journal of King Saud University - Science*, 2016, 30: 168–175. <https://doi.org/10.1016/j.jksus.2016.10.002>
- [21] G. Rajakumar, M. Thiruvengadam, G. Mydhili, et al. Green approach for synthesis of zinc oxide nanoparticles from *Andrographis paniculata* leaf extract and evaluation of their antioxidant, anti-diabetic, and anti-inflammatory activities. *Bioprocess and Biosystems Engineering*, 2018, 41(10): 21–30. <https://doi.org/10.1007/s00449-017-1840-9>
- [22] J. Singh, S. Kumar, A. Alok, et al. The potential of green synthesized zinc oxide nanoparticles as nutrient source for plant growth. *Journal of Cleaner Production*, 2019, 214: 1061–1070. <https://doi.org/10.1016/j.jclepro.2019.01.018>
- [23] J. Li, Y. Li, H.S. Wu, et al. Facile synthesis of ZnO nanoparticles by *Actinidia deliciosa* fruit peel extract: Bactericidal, anticancer and detoxification properties. *Environmental Research*, 2021, 200: 111433. <https://doi.org/10.1016/j.envres.2021.111433>
- [24] J. Ruangtong, J. T-Thienprasert, N.P. T-Thienprasert. Green synthesized ZnO nanosheets from banana peel extract possess anti-bacterial activity and anti-cancer activity. *Materials Today Communications*, 2020, 24: 101224. <https://doi.org/10.1016/j.mtcomm.2020.101224>
- [25] Y.L. Gao, D. Xu, D. Ren, et al. Green synthesis of zinc oxide nanoparticles using *Citrus sinensis* peel extract and application to strawberry preservation: A comparison study. *LWT*, 2020, 126: 109297. <https://doi.org/10.1016/j.lwt.2020.109297>
- [26] M. Aminuzzaman, P.S. Ng, W. Goh, et al. Value-adding to dragon fruit (*Hylocereus polyrhizus*) peel biowaste: Green synthesis of ZnO nanoparticles and their characterization. *Inorganic and Nano-Metal Chemistry*, 2019, 49(11): 401–411. <https://doi.org/10.1080/24701556.2019.1661464>
- [27] B. Vishnupriya, G.R. Elakkiya Nandhini, G. Anbarasi, Biosynthesis of zinc oxide nanoparticles using *Hylocereus undatus* fruit peel extract against clinical pathogens, *Materials Today: Proceedings*, 2022, 48(2): 164–168. <https://doi.org/10.1016/j.matpr.2020.05.474>
- [28] E.J. Rupa, G. Anandapadmanaban, R. Mathiyalagan, et al. Synthesis of zinc oxide nanoparticles from immature fruits of *Rubus coreanus* and its catalytic activity for degradation of industrial dye. *Optik*, 2018, 172: 1179–1186. <https://doi.org/10.1016/j.jileo.2018.07.115>
- [29] F. Shao, A.J. Yang, D.M. Yu, et al. Biosynthesis of *Barleria gibsoni* leaf extract mediated zinc oxide nanoparticles and their formulation gel wound therapy in nursing care of infants and children. *Journal of Photochemistry and Photobiology B: Biology*, 2018, 189: 267–273. <https://doi.org/10.1016/j.jphotobiol.2018.10.014>
- [30] A.L. Hanna, H.M. Hamouda, H.A. Goda, et al. Biosynthesis and characterization of silver nanoparticles produced by *Phormidium ambiguum* and *Desertifilum tharense* cyanobacteria. *Bioinorganic Chemistry and Applications*, 2022, 2022: 9072508. <https://doi.org/10.1155/2022/9072508>
- [31] H. Agarwal, S. Menon, K.S. Venkat, et al. Phyto-assisted synthesis of zinc oxide nanoparticles using *Cassia alata* and its antibacterial activity against *Escherichia coli*. *Biochemistry and Biophysics Reports*, 2019, 17: 208–211. <https://doi.org/10.1016/j.bbrep.2019.01.002>
- [32] S. Vijayakumar, B. Vaseeharan, B. Malaikozhundan, et al. *Laurus nobilis* leaf extract mediated green synthesis of ZnO nanoparticles: Characterization and biomedical applications. *Biomedicine & Pharmacotherapy*, 2016, 84: 1213–1222. <https://doi.org/10.1016/j.biopha.2016.10.038>
- [33] H. Çolak, E. Karaköse, Green synthesis and characterization of nanostructured ZnO thin films using *Citrus aurantifolia* (lemon) peel extract by spin-coating method. *Journal of Alloys and Compounds*, 2017, 690: 658–662. <https://doi.org/10.1016/j.jallcom.2016.08.090>
- [34] G. Madhumitha, J. Fowsiya, N. Gupta, et al. Green synthesis, characterization and antifungal and photocatalytic activity of *Pithecellobium dulce* peel-mediated ZnO nanoparticles. *Journal of Physics and Chemistry of Solids*, 2019, 127: 43–51. <https://doi.org/10.1016/j.jpics.2018.12.005>
- [35] D. Titus, E. James Jebaseelan Samuel, S.M. Roopan. Nanoparticle characterization techniques. *Green Synthesis, Characterization and Applications of Nanoparticles*. Amsterdam: Elsevier, 2019: 303–319. <https://doi.org/10.1016/j.elsevier.2019.303-319>

- 1016/B978-0-08-102579-6.00012-5
- [36] J. Ali, R. Irshad, B.S. Li, et al. Synthesis and characterization of phytochemical fabricated zinc oxide nanoparticles with enhanced antibacterial and catalytic applications. *Journal of Photochemistry and Photobiology B: Biology*, 2018, 183: 349–356. <https://doi.org/10.1016/j.jphotobiol.2018.05.006>
- [37] A. Chahardoli, N. Karimi, F. Sadeghi, et al. Green approach for synthesis of gold nanoparticles from *Nigella arvensis* leaf extract and evaluation of their antibacterial, antioxidant, cytotoxicity and catalytic activities. *Artificial Cells, Nanomedicine, and Biotechnology*, 2018, 46(3): 579–588. <https://doi.org/10.1080/21691401.2017.1332634>
- [38] J.R. Nakkala, E. Bhagat, K. Suchiang, et al. Comparative study of antioxidant and catalytic activity of silver and gold nanoparticles synthesized from *Costus pictus* leaf extract. *Journal of Materials Science & Technology*, 2015, 31(10): 986–994. <https://doi.org/10.1016/j.jmst.2015.07.002>
- [39] L. David, B. Moldovan. Green synthesis of biogenic silver nanoparticles for efficient catalytic removal of harmful organic dyes. *Nanomaterials*, 2020, 10(2): 202. <https://doi.org/10.3390/nano10020202>
- [40] F.S. Rosarin, V. Arulmozhi, S. Nagarajan, et al. Antiproliferative effect of silver nanoparticles synthesized using amla on Hep2 cell line. *Asian Pacific Journal of Tropical Medicine*, 2013, 6(1): 1–10. [https://doi.org/10.1016/S1995-7645\(12\)60193-X](https://doi.org/10.1016/S1995-7645(12)60193-X)
- [41] J.G. Heddle. Gold nanoparticle-biological molecule interactions and catalysis. *Catalysts*, 2013, 3(3): 683–708. <https://doi.org/10.3390/catal3030683>
- © The author(s) 2023. This is an open-access article distributed under the terms of the Creative Commons Attribution 4.0 International License (CC BY) (<http://creativecommons.org/licenses/by/4.0/>), which permits unrestricted use, distribution, and reproduction in any medium, provided the original author and source are credited.